

# Activation of Bestrophin Cl<sup>-</sup> Channels Is Regulated by C-terminal Domains\*

Received for publication, February 2, 2007, and in revised form, April 10, 2007. Published, JBC Papers in Press, April 17, 2007, DOI 10.1074/jbc.M701043200

Zhi Qiang Qu<sup>1</sup>, Kuai Yu, Yuan Yuan Cui, Carl Ying, and Criss Hartzell

From the Department of Cell Biology and Center for Neurodegenerative Disease, Emory University School of Medicine, Atlanta, Georgia 30322

Bestrophins (VMD2, VMD2L1, VMD2L2, and VMD2L3) are a new family of anion channels. The mechanisms of their regulation are not yet well understood. Recently, we found that a domain (amino acids 356–364) in the C terminus of mouse VMD2L3 (mBest3) inhibited channel activity when it was expressed in HEK293 cells (Qu, Z., Cui, Y., and Hartzell, H. C. (2006) *FEBS Lett.* 580, 2141–2214). Here we show that this auto-inhibitory (AI) domain in mBest3 and human (h)Best3 is composed of seven critical residues, <sup>356</sup>IPSFGLS<sup>362</sup>. Replacement of any residue (except Pro<sup>357</sup>) in the domain with alanine activated Cl<sup>-</sup> currents. Substitution of Pro<sup>357</sup> with other amino acids, especially phenylalanine, did activate currents. Membrane biotinylation demonstrated that nonfunctional mBest3 protein was trafficked to the plasma membrane, implying that the AI domain inhibited channel gating but not trafficking. mBest3-F359A and hBest3-G361A mutations induced outwardly rectifying currents, suggesting that the AI domain is associated with the channel pore or gating mechanism. Supporting this suggestion, the mBest3 AI domain was demonstrated to be located within a membrane-associated region. When the wild-type mBest3 C terminus (amino acids 292–669) was expressed in HEK293 cells, the protein was located mainly in the particulate fraction, but it became soluble when a sequence containing the AI domain was deleted ( $\Delta$ 353–404). There is an AI domain (<sup>357</sup>QPSFQGS<sup>363</sup>) in mouse VMD2L1 (mBest2) as well, but its inhibitory effect is competed by a downstream facilitatory sequence (amino acids 405–454). These results suggest that an auto-inhibitory mechanism in C termini may be universal among bestrophins investigated in the study.

Bestrophins are a new family of Cl<sup>-</sup> channels, some of which are sensitive to intracellular Ca<sup>2+</sup> (2–6). There are four bestrophin genes in humans but three in mice, and there may be several alternatively spliced forms of bestrophins in the two species (7–9). Human VMD2 (human bestrophin 1 or hBest1)<sup>2</sup>

has been recognized as a gene responsible for inherited Best vitelliform macular dystrophy (8, 10). However, the tissue-specific functions of other three members remain poorly understood. Recently, there has been significant progress in uncovering the physiological functions of bestrophins. Using an RNAi strategy, Hartzell and co-workers (11) demonstrated that bestrophins represent the endogenous Ca<sup>2+</sup>-dependent Cl<sup>-</sup> channels in *Drosophila* S2 cells. S2 cells express four bestrophins (dbest1–4). The endogenous CaCl current (I<sub>CaCl</sub>) was abolished by RNAi to dbest1 or dbest2 but not to dbest3 or dbest4, suggesting that the endogenous CaCl channel is composed of a heteromer of dbest1 and dbest2. Also with an RNAi approach, Kunzelmann and co-workers (12) showed that hBest1 was the molecular counterpart of the Ca<sup>2+</sup>-activated Cl<sup>-</sup> current (I<sub>CaCl</sub>) in epithelial tissues. Native I<sub>CaCl</sub> coincided with endogenous expression of hBest1 in 16HBE cells, but the current was absent in H441 cells that did not express hBest1 protein. Blocking expression of hBest1 in HT<sub>29</sub> human colonic epithelial cells with short interfering RNA suppressed the whole-cell I<sub>CaCl</sub> induced by extracellular ATP application (which raises intracellular Ca<sup>2+</sup> concentration). Furthermore, it has been suggested that the I<sub>CaCl</sub> in olfactory sensory neurons (OSNs), which is important in amplification of olfactory transduction, is mediated by mouse VMD2L1 (mBest2) (13). By single-cell reverse transcription-PCR, mBest2 was found to be expressed in OSNs but not in supporting cells. By immunocytochemistry, mBest2 was localized on the cilia of OSNs and colocalized with the CNGA2 channel subunit. Electrophysiological properties of I<sub>CaCl</sub> in dendritic knob/cilia of mouse OSNs were comparable with those induced by mBest2 expression in HEK293 cells. Therefore, the authors suggest that mBest2 is a molecular component of the olfactory CaCl channel.

Despite rapid progress in the molecular characterization of bestrophins, not much is known about their regulation. We do not know how they are activated by Ca<sup>2+</sup> or how their intra- or extracellular domains regulate channel function. Although hBest1, hBest2, hBest4, and mBest2 have been shown to function as CaCl channels in heterologous expression systems, hBest3 and mBest3<sup>3</sup> did not induce significant currents within a physiological voltage range (1, 6). This phenomenon prompted

\* This work was supported by American Heart Association (Scientist Development Grant), Emory CHA Pilot Grant, American Federation of Aging Research Award (to Z. Q.), and National Institutes of Health Grants GM60448 and EY014852 (to C. H.). The costs of publication of this article were defrayed in part by the payment of page charges. This article must therefore be hereby marked "advertisement" in accordance with 18 U.S.C. Section 1734 solely to indicate this fact.

<sup>1</sup> To whom correspondence should be addressed: Dept. of Cell Biology, Emory University School of Medicine, 615 Michael St., 535 Whitehead Bldg., Atlanta, GA 30322-3030. Tel.: 404-727-6260; Fax: 404-727-6256; E-mail: zqu@emory.edu.

<sup>2</sup> The abbreviations used are: hBest1, human bestrophin 1; VMD, vitelliform macular dystrophy; VMD2L, vitelliform macular dystrophy 2 like; mBest2, mouse VMD2L1; mBest3, mouse VMD2L3; hBest3, human VMD2L3; HEK,

human embryonic kidney; TMD, transmembrane domain; OSN, olfactory sensory neuron; AI, auto-inhibitory; GAPDH, glyceraldehyde-3-phosphate dehydrogenase; PBS, phosphate-buffered saline; RNAi, RNA interference.

<sup>3</sup> Mouse VMD2L3 was named as mBest4 in our previous publication (1). According to the bestrophin nomenclature by the HUGO gene (HGNC: 17105) and the Mouse Genome Database nomenclature committees (MGI: 3580298), mouse VMD2L3 has been corrected to mBest3 (17).

us to search for regulatory domains in the C terminus of the Best3 proteins. We found an auto-inhibitory (AI) domain in the mBest3 C terminus, which turned off the channel. We narrowed the AI domain to the <sup>356</sup>IPSFLGSTI<sup>364</sup> sequence (1). In this study, we have investigated further the function of the AI domain. We found that the AI domain of mBest3 is membrane-associated. An AI domain was also identified to be present in mBest2, which is competed by a downstream stimulatory sequence. Therefore, we suggest that the AI domain may be a common mechanism for the channel regulation of the bestrophins we have studied.

## EXPERIMENTAL PROCEDURES

**Generation of Bestrophin Mutations and Heterologous Expression**—mBest2 (mouse VMD2L1) in pSPORT6 expression vector was obtained from the ATCC (2). mBest3 (mouse VMD2L3) cDNA was cloned by reverse transcription-PCR and subcloned into pcDNA3.1 (1). hBest3 (human VMD2L3) was obtained from Dr. Jeremy Nathans (The Johns Hopkins University) (6). Site-specific mutations were generated using a PCR-based mutagenesis kit (Quickchange, Stratagene) as described previously (2). The cDNA expression vectors were co-transfected with pEGFP (Invitrogen) into HEK293 cells (ATCC) using FuGENE 6 transfection reagent (Roche Applied Science). The transfected cells were identified by the pEGFP-expressed green fluorescence. The transfection efficiency was 20–30%. 0.1–0.3 μg of plasmid was used to transfect HEK293 cells on one 35-mm culture dish. The next day, cells were trypsinized and placed on the coverslips for electrophysiological recording.

**Electrophysiology**—Recordings were performed at 22–24 °C using the whole-cell configuration of the patch clamp (14). Voltage steps were used as indicated in the figure legends with a holding potential of 0 mV. The standard pipette solution (~4.5 μM free Ca<sup>2+</sup>) contained (in mM) 146 CsCl, 2 MgCl<sub>2</sub>, 5 (Ca<sup>2+</sup>)-EGTA, 10 sucrose, 8 HEPES, pH 7.3 (2). The standard extracellular solution contained (in mM) 140 NaCl, 4 KCl, 2 CaCl<sub>2</sub>, 1 MgCl<sub>2</sub>, 10 glucose, 10 HEPES, pH 7.3. This combination of solutions set  $E_{rev}$  for Cl<sup>-</sup> currents to zero, whereas cation currents carried by Na<sup>+</sup> or Cs<sup>+</sup> had very positive or negative  $E_{rev}$ , respectively (2). To verify the currents were carried by Cl<sup>-</sup>, cells were exposed to a solution containing 100 mM Na<sub>2</sub>SO<sub>4</sub>, 1 mM CaCl<sub>2</sub>, 10 mM HEPES, pH 7.3. Because SO<sub>4</sub> is not permeant through bestrophin channels, this solution blocked outward current, if it was carried by bestrophin channels. The amplitude of whole-cell currents at the end of 100-mV pulse was measured and is shown as mean ± S.E. The Student's *t* test was used for statistical analysis.

**Development of a Polyclonal Antibody to mBest3**—The cDNA encoding the last 200 amino acids of the mBest3 C terminus was subcloned into pET-28a vector to produce a hexahistidine-tagged protein. The protein was purified on nickel-nitrilotriacetic His-Bind resin (Novagen) and used to raise the polyclonal antibody to mBest3 in rabbits. The anti-mBest3 antibody (05619) recognizes mBest3 specifically. For Western blotting, 1/2000 dilution was used, but 1/1000 was used for immunocytochemistry.

**Biotinylation of the Proteins on the Plasma Membrane Surface**—The mBest3 proteins in the plasma membrane of HEK293 cells were examined with membrane biotinylation, affinity purification, and Western blotting. Membrane surface biotinylation has been described previously (12). Briefly, transfected and native HEK293 cells were exposed to the membrane-impermeable Sulfo-NHS-LC biotin for 30 min at 4 °C. The biotinylated membrane proteins were solubilized and affinity-purified with streptavidin beads. The purified proteins were subjected to Western blotting probed with the antibody to mBest3 (05619) (1/2000 dilution) followed by horseradish peroxidase-conjugated goat anti-rabbit IgG (1/3000 dilution) (Jackson ImmunoResearch). Anti-GAPDH (a cytoplasmic protein) antibody was used to probe immunoblots to indicate the specificity of membrane protein biotinylation.

**Solubility of Bestrophin C Termini**—mBest3 C-terminal domains, 292–669 or 292–669(Δ353–404) cDNA, subcloned in the pcDNA3.1 vector (1) were transfected into HEK293 cells with Lipofectamine 2000 (Invitrogen). The transfection efficiency was about 60%. The transfected cells were harvested 2 days after transfection, sonicated briefly in phosphate-buffered saline (PBS) containing 1 mM dithiothreitol, 1 mM phenylmethylsulfonyl fluoride, and 1/200 (volume) protease inhibitor set III (Calbiochem), and ultracentrifuged at 42,500 × *g* (Beckman Optima TLX ultracentrifuge, TLS 55 rotor). The supernatant was collected as a soluble fraction. The pellet was washed with PBS, dissolved in a nonionic detergent lysis buffer (mM) (1% Triton X-100, 150 NaCl, 0.5 EGTA, 10% glycerol, 1 dithiothreitol, 10 HEPES, pH 7.3, 1 phenylmethylsulfonyl fluoride, 1/200 protease inhibitor mixture III), and centrifuged at 16,000 × *g*. The supernatant contained the Triton-soluble membrane proteins. Protein concentrations were measured with the BCA Protein Assay kit (Pierce). Western blotting was performed with equivalent amounts (10 μg/lane) of protein from each sample. mBest3 C termini were detected with the anti-mBest3 antibody (05619) followed by horseradish peroxidase-conjugated goat anti-rabbit Ig G and chemiluminescence.

## RESULTS

**The Auto-inhibitory (AI) Domain in mBest3 or hBest3 Is Composed of Seven Residues**—In our previous study, we showed that a domain in the C terminus of mBest3 inhibited its channel activity. By deletion or mutation of groups of amino acids, we localized the AI domain to nine residues (<sup>356</sup>IPSFLGSTI<sup>364</sup>) (1). To determine which residues are responsible for the inhibition, we individually mutated each residue in the domain to alanine. Alanine substitution of residues 356 and 358–362 activated the mBest3 channel (Fig. 1A), whereas the D353A, Y354A, C355A, P357A, T363A, I364A, and Gln<sup>365</sup> mutations were not effective in activating mBest3. hBest3 (6) is 86% identical to mBest3 (see alignment in Fig. 8A). It possesses an AI domain (*boldface letters* in Fig. 8A) identical to that of mBest3. Neither hBest3 nor mBest3 induced significant Cl<sup>-</sup> currents in HEK293 cells with voltage pulses in a physiological range (1, 6). Therefore, we hypothesized that both channels share the same mechanism for their activation. As expected, mutation of the homologous residues in hBest3 AI domain activated the channel as well (Fig. 1B).

## Regulation of Bestrophin Cl<sup>-</sup> Channel Activation

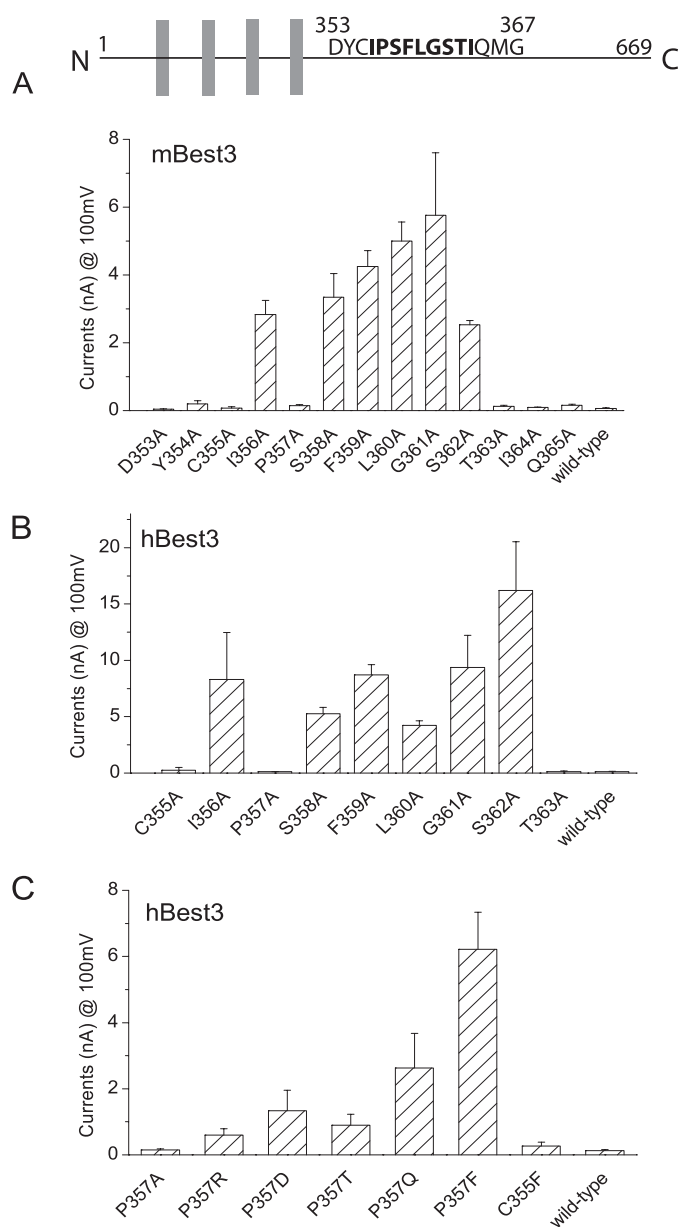


**FIGURE 1. Critical residues in the AI domains responsible for mBest3 and hBest3 activation.** Upper panel shows a schematic of mBest3 where seven boldface italic letters indicate the AI domain. AI domain mutants were transfected into HEK cells which were whole-cell voltage clamped with high  $[Ca^{2+}]_i$  in the pipette. Voltage steps were applied in 20-mV increments between  $-100$  and  $100$  mV for 1 or 3 s. Internal and external solutions were described under "Experimental Procedures." Average amplitudes of Cl<sup>-</sup> currents at the end of the  $+100$ -mV trace are shown. *A*, effect of alanine substitution on mBest3 channel activation. The current amplitudes of I356A, S358A, F359A, L360A, G361A, and S362A mutants were dramatically increased, compared with wild-type mBest3 ( $p < 0.01$ ,  $n = 4-7$ ). Other mutations did not significantly change the channel activity. *B*, effect of mutations in the AI domain on hBest3 channel activation. As with mBest3, I356A, S358A, F359A, L360A, G361A, and S362A significantly activated the hBest3 channels. Their activities were statistically higher than wild-type hBest3 ( $p < 0.01$ ,  $n = 4-5$ ). *C*, effects of various mutations at position 357 on hBest3 channel activation. P357F mutation activated the wild-type hBest3 channel ( $p < 0.01$ ) more than P357R, P357D, P357T, or P357Q mutations ( $p < 0.05$ ) ( $n = 4-10$ ).

The finding that the P357A mutation did not activate mBest3 or hBest3 currents can be interpreted as evidence that Pro<sup>357</sup> has no role in channel inhibition or, alternatively, that the P357A mutant was nonfunctional for another reason, such as

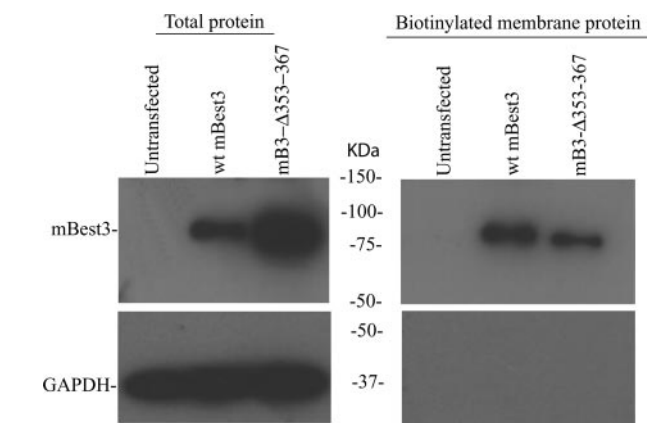


**FIGURE 2. mBest3 proteins are expressed in the plasma membrane.** Wild-type (wt) mBest3,  $\Delta 353-367$ , or G361A mutant-transfected and nontransfected HEK293 cells were exposed to the membrane-impermeable sulfo-NHS-LC biotin for 30 min at  $4^\circ C$ . The biotinylated membrane proteins were affinity-purified with streptavidin resin. The purified proteins were subjected to Western blotting with an antibody to mBest3 (upper panels). GAPDH (a cytoplasmic protein, detected with an antibody to GAPDH in the lower panels) was not biotinylated, indicating the specificity of the membrane protein biotinylation (see "Experimental Procedures" for details).

protein mis-folding. Because proline residues often play important roles in protein secondary structure and Pro<sup>357</sup> is flanked by residues that are important in the AI domain, we tested the possibility that substituting other amino acids for Pro<sup>357</sup> might activate the channel. Substitution of Pro<sup>357</sup> with Arg, Asp, Thr, and Gln resulted in small but distinct currents (Fig. 1C). The P357F mutation produced large currents. To test the specificity of the Pro to Phe mutation, we mutated Cys<sup>355</sup> into Phe because the C355A mutant was nonfunctional (Fig. 1, A and B) and Cys<sup>355</sup> is just one amino acid away from Pro<sup>357</sup>. The C355F mutation did not activate significant current (Fig. 1C), indicating that the effect of the P357F mutation on hBest3 is specific. Without a tertiary structure of VMD2L3, we do not have an explanation why the Phe but not the Ala substitution activates hBest3 currents, but these data show that Pro<sup>357</sup> is also a critical residue for the inhibitory effect of the AI domain.

**mBest3 Is Trafficked to the Plasma Membrane**—The observation that wild-type mBest3 and hBest3 did not evoke significant Cl<sup>-</sup> currents under physiological conditions could be explained by two mechanisms. The AI domain could block the channel in the plasma membrane by interacting with the channel pore or channel gating machinery, or the AI domain could prevent the channel protein from trafficking properly to the plasma membrane. To clarify the uncertainty, we developed an antibody to the last 200 amino acids of the mBest3 C terminus. This antibody recognizes a single protein band of  $\sim 80$  kDa from HEK cells expressing mBest3. This value is close to the calculated mBest3 molecular mass of 78 kDa (upper panels in Fig. 2). The band was absent in nontransfected HEK cells. To determine whether wild-type mBest3 was expressed in the plasma membrane, we biotinylated plasma membrane proteins with a membrane-impermeant biotinylation reagent and then examined the presence of mBest3 with the anti-mBest3 antibody. Fig. 2 shows that both the nonfunctional mBest3 and its functional mutant, mB3( $\Delta 353-367$ ) were located in the plasma membrane of HEK293 cells. The results strongly suggest that

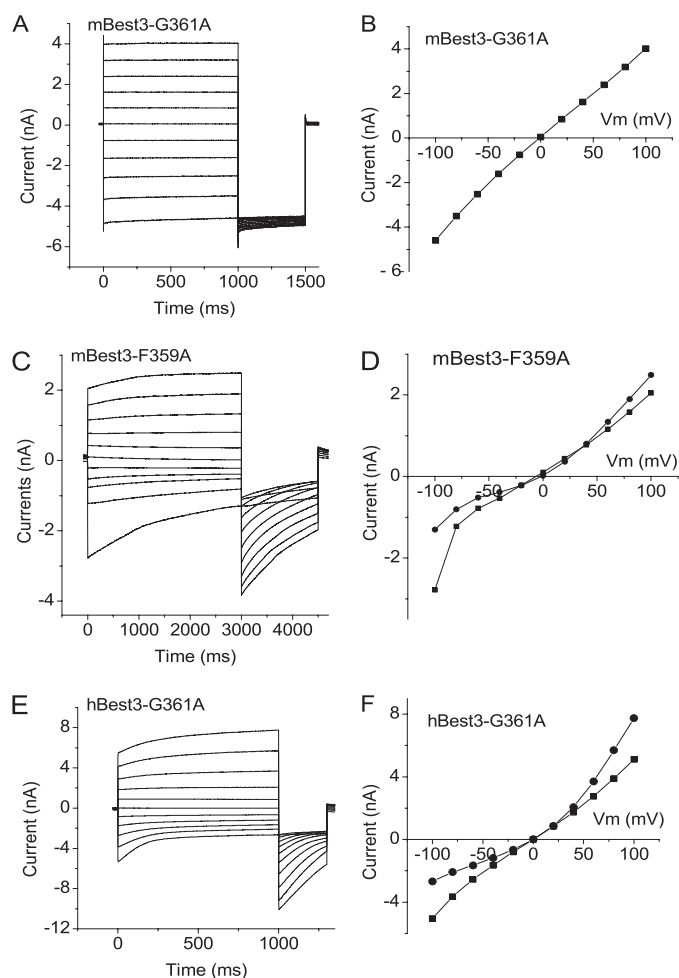


**FIGURE 3. Certain mutations in mBest3 and hBest3 AI domains alter kinetics of activation.** Whole-cell recordings were performed as described in Fig. 1. *A*, *C*, and *E*, current traces. *B*, *D*, and *F*, current-voltage relationships of currents at the start (■) and end (●) of the voltage pulses in *A* and *B*. mBest3-G361A ( $n = 5$ ). Currents are time- and voltage-independent. *C* and *D*, mBest3-F359A. Currents are time- and voltage-dependent with slow tail current deactivation ( $n = 7$ ). *E* and *F*, hBest3-G361A. Currents are time- and voltage-dependent currents with fast tail current deactivation ( $n = 4$ ).

the inactivation of mBest3 by the AI domain occurs via inhibition of channel permeation or gating.

**Certain AI Domain Mutations Alter Channel Gating**—Most of the currents that were induced by AI domain mutations in mBest3 or hBest3 were time- and voltage-independent. The mBest3-G361A mutation is shown as an example (Fig. 3, *A* and *B*). However, the F359A mutation in mBest3 (Fig. 3, *C* and *D*) and the G361A mutation in hBest3 (Fig. 3, *E* and *F*) induced currents that exhibited both time and voltage dependence. The currents were outwardly rectifying. This outward rectification was apparently a consequence of voltage-dependent closure of the channels at negative membrane potentials as evidenced by the time-dependent deactivation of the current at negative potentials. Interestingly, the deactivation kinetics of hBest3-G361A at negative potentials was much faster than deactivation of mBest3-F357A. The time constant of deactivation of the current upon repolarization to  $-100$  from  $0$  mV was  $573.5 \pm 225.1$  ms ( $n = 4$ ) for hBest3-G361A, but it was more than five times slower ( $3038.9 \pm 549.6$  ms,  $n = 7$ ) for mBest3-F359A ( $p = 0.01$ ). The effect of these mutations on the voltage and time depend-

ence of the current supports the idea that the AI domain associates with the channel pore or gating mechanism. I-V relationships indicate that the currents induced by the above mutations were carried by Cl<sup>-</sup> anions because the  $V_{rev}$  was close to  $E_{Cl}$  ( $0$  mV) for each mutation (Fig. 3 *B*, *D*, and *F*), implying that the mutations did not change the anion/cation selectivity of the Best3 channels. We have not tested, however, whether they change relative anion permeability.

Cysteine mutations of the pore residues have been useful for dissecting the pore structure of bestrophins (6, 15). In an attempt to understand better the structure of the AI domain, we substituted Phe<sup>359</sup> in mBest3 and Gly<sup>361</sup> in hBest3 with cysteines. Unlike the alanine mutations, both cysteine substitutions (F359C and G361C) activated time- and voltage-independent whole-cell currents (data not shown). The membrane-permeable (2-aminoethyl)methanethiosulfonate hydrobromide (MTSEA<sup>+</sup>) or membrane-impermeable [2-(trimethylammonium)ethyl]-methanethiosulfonate bromide (MTSET<sup>+</sup>) and (2-sulfonatoethyl)methanethiosulfonate (MTSES<sup>-</sup>) (1 mM) applied extracellularly did not alter current amplitude or wave form (data not shown). The negative results can be interpreted by the possibility that the polar cysteine at position 359 (mBest3) or 361 (hBest3) may have already driven the AI domain dissociate from the pore structure, rendering the channel unresponsive to methanethiosulfonate reagent modification (see below).

**The AI Domain Is Membrane-associated**—The result that certain mutations in the AI domain apparently affected the channel gating invited us to examine mBest3 topology to see if the AI domain is a membrane-associated structure. Hydrophathy analysis by the MPEx program shows that the sequence, <sup>355</sup>CIPSEFLGSGTIQMGLSGSNF<sup>373</sup>, including the AI domain (underlined), is more hydrophobic than the surrounding sequence, although it is not predicted to be a TMD (Fig. 4*A*). To test whether the AI domain is membrane-associated, we measured the association of the mBest3 wild-type or the AI domain-deleted mutant C terminus with the membrane. The mBest3 wild-type C terminus (amino acids 292–668) or the C-terminal mutant, 292–668( $\Delta$ 353–404), in which amino acids 353–404, including the AI domain were deleted, was overexpressed in HEK293 cells, respectively. The cells were disrupted by sonication in PBS. The extract was ultracentrifuged to separate soluble (S) and particulate fractions. Then the particulate fraction was suspended in buffer containing 1% Triton X-100 to solubilize membrane proteins. The high speed supernatant from this extract contained membrane proteins. Proteins from soluble or membrane fractions were subjected to SDS-PAGE and Western blotting probed with the anti-mBest3 antibody (Fig. 4*B*). The wild-type C terminus (292–668) was detected predominantly in the membrane fraction (Fig. 4*B*, *M*, lane 2), whereas the distribution of the C-terminal mutant, 292–668( $\Delta$ 353–404), was in the soluble fraction (S, lane 3). The result strongly suggests that a region of the mBest3 C terminus that includes the AI domain is membrane-associated. Based on the suggestion, we assume that the AI domain may block the channel pore via binding to its “receptor” in a relatively hydrophobic environment of the plasma membrane.

## Regulation of Bestrophin Cl<sup>-</sup> Channel Activation

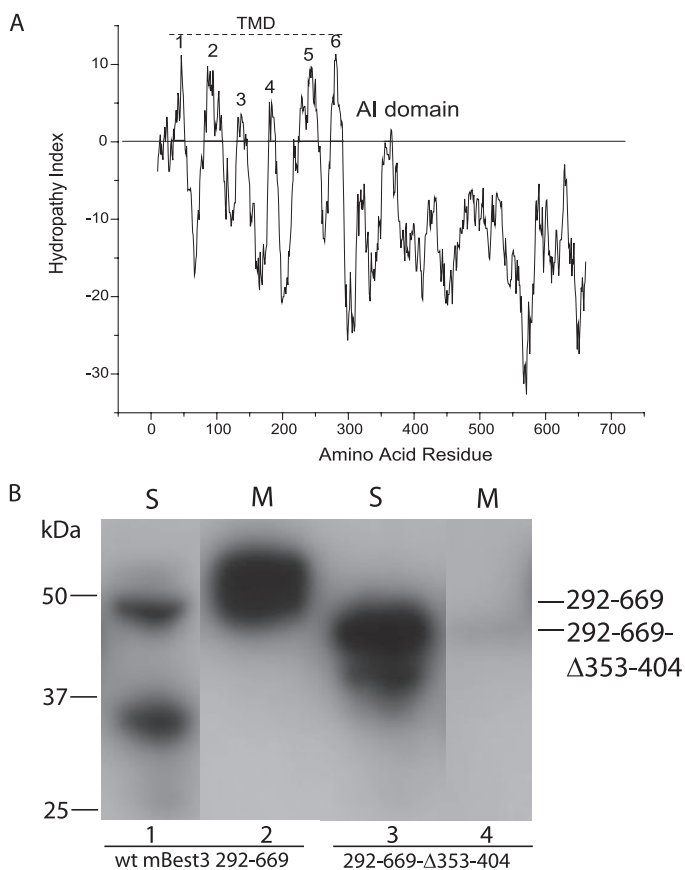


**FIGURE 4. The mBest3 AI domain is probably membrane-associated.** *A*, hydropathy analysis of mBest3 with MPEX program. Six potential TMDs are predicted. *B*, deletion of residues 353–404 increased the solubility of the mBest3 C terminus. Wild-type mBest3 C terminus with residues 292–668 (lanes 1 and 2) or C terminus with residues 353–404 deleted (lanes 3 and 4) was transfected into HEK293 cells. The proteins in soluble (S) and membrane (M) fractions were extracted as described under “Experimental Procedures” and subjected to SDS-PAGE and Western blotting with the anti-mBest3 antibody. The bands with smaller molecular masses in lanes 1 and 3 were probably the protease-degraded proteins.

**Introduction of the mBest3 AI Domain into mBest2 Does Not Inactivate the Channel**—The region homologous to the mBest3 AI domain in mBest2 differs from mBest3 by only two amino acids (<sup>357</sup>QPSFQGS<sup>363</sup> for mBest2, <sup>356</sup>IPSFLGS<sup>362</sup> for mBest3) (1). Because wild-type mBest2 is functional as a Cl<sup>-</sup> channel in HEK293 cells, we hypothesized that the difference in functionality of mBest2 and mBest3 was because of the two different amino acids. To test the hypothesis, we changed the <sup>357</sup>QPSFQGS<sup>363</sup> sequence in mBest2 to that of the mBest3 AI domain, IPSFLGS. We expected that this change would inactivate mBest2. However, unexpectedly, the Cl<sup>-</sup> current amplitude in the mBest2-Q357I/Q361L mutant was dramatically enhanced (Fig. 5). The single mutations Q357I, Q361L, or Q361A in mBest2 also significantly facilitated the Cl<sup>-</sup> current. These results suggest that <sup>357</sup>QPSFQGS<sup>363</sup> domain is probably an AI domain in mBest2 and functions to inhibit the channel activity, but its efficacy may be suppressed by other domains having facilitatory functions. Once the inhibitory structure of the AI domain is disrupted by mutations, the channel activity is augmented by the facilitatory domain.

**A Facilitatory Structure in the C Terminus of mBest2 Suppresses the Efficacy of Its AI Domain**—To explain why the AI domain of mBest2 cannot completely inhibit the Cl<sup>-</sup> channel,

we hypothesized that there might be other sequences existent in mBest2 that can suppress or compete the function of its AI domain. In an attempt to locate such a hypothetical domain, we truncated mBest2 at Leu<sup>294</sup>, Phe<sup>353</sup>, Val<sup>405</sup>, or Ser<sup>454</sup> by introducing a stop codon (X) (Fig. 6C, upper panel). L294X(Δ294–508) and V405X(Δ405–508) were nonfunctional, whereas F353X(Δ353–508) and S454X(Δ454–508) were functional (Fig. 6, A–C). The currents induced by F353X and S454X were similar to wild-type mBest2 (Fig. 6B), both time- and voltage-independent (2). The nonfunctionality of L294X is consistent with the idea that the well conserved sequence (amino acids 294–353) immediately after the last predicted TMD is essential for mBest2 channel function. Deletion of the C terminus starting with the AI domain (F353X) resulted in currents that were similar in amplitude to the wild-type mBest2 currents but smaller than mBest2-Q361A currents (Fig. 5). The data from the Q361A mutation and the F353X mutation taken together suggest that in addition to the AI domain, mBest2 may have another structure in the C terminus that facilitates the current amplitude. The nonfunctionality of F405X and functionality of S454X indicates that this facilitatory structure is located between amino acids 405 and 454. We hypothesized that nonfunctionality of the V405X mBest2 channel was because of inhibition of the channel by the AI domain in the absence of the facilitatory structure. To test this idea, residues 356–364 in and flanking the AI domain of the V405X(Δ405–508) mutant were substituted with alanines individually. Mutation of each of the residues except Q356A, P358A, and T364A stimulated the V405X current (Fig. 6D). These data show that an AI domain does exist in mBest2 and suggest that the current amplitude of mBest2 is determined by the competition between the AI domain (residues 357–363) and a facilitatory domain located within the region bounded by the residues 405 and 454.

**The Facilitatory Region (Residues 405–454) of mBest2 Is Functional in mBest3**—To test the functionality of the region (residues 405–454) of mBest2 in other bestrophins, we swapped the corresponding residues 405–454 between mBest2 and mBest3. As shown in Fig. 7A, when the residues 405–454 of mBest3 were replaced with the residues 405–454 from mBest2, the mBest3 channel was activated, suggesting that the region (residues 405–454) of mBest2 is also functional in mBest3 as a facilitatory structure. To test the function of the residues 405–454 of mBest3, the residues 405–454 in mBest2 were replaced with the corresponding residues from mBest3. Consequently, the wild-type mBest2 channel activity was significantly reduced by about 70% (Fig. 7B), indicating that the residues 405–454 of mBest3 has much less facilitatory function than the matching sequence (405–454) in mBest2.

## DISCUSSION

This study shows that the activation of three bestrophin channels is regulated by a similar mechanism; a membrane-associated AI domain in the C terminus inhibits channel activity. The AI domain consists of seven amino acids. Each residue in the domain when mutated individually can activate or enhance the activities of the channels. The inhibitory effect exerted on the bestrophins is assumed to occur at the plasma membrane. Although the mechanism for the AI domain action

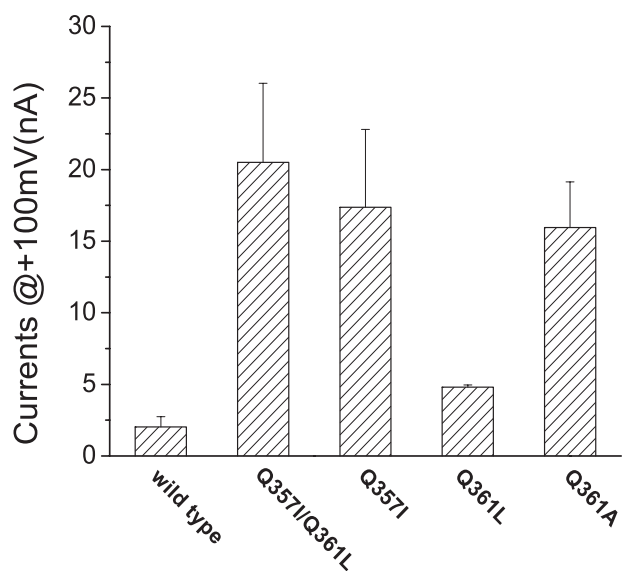


**FIGURE 5. Introduction of mBest3 AI domain facilitated rather than inhibited the mBest2 channel.** Whole-cell recordings were performed on the mutant mBest2-transfected HEK293 cells as described in Fig. 1. The mBest3 AI domain has been introduced into mBest2 by the Q357I/Q361L mutations. The introduction of mBest3 AI domain facilitated the mBest2 currents. All mutations shown in this figure induced significantly larger currents than wild-type mBest2 ( $p < 0.01$ ,  $n = 4-11$ ).

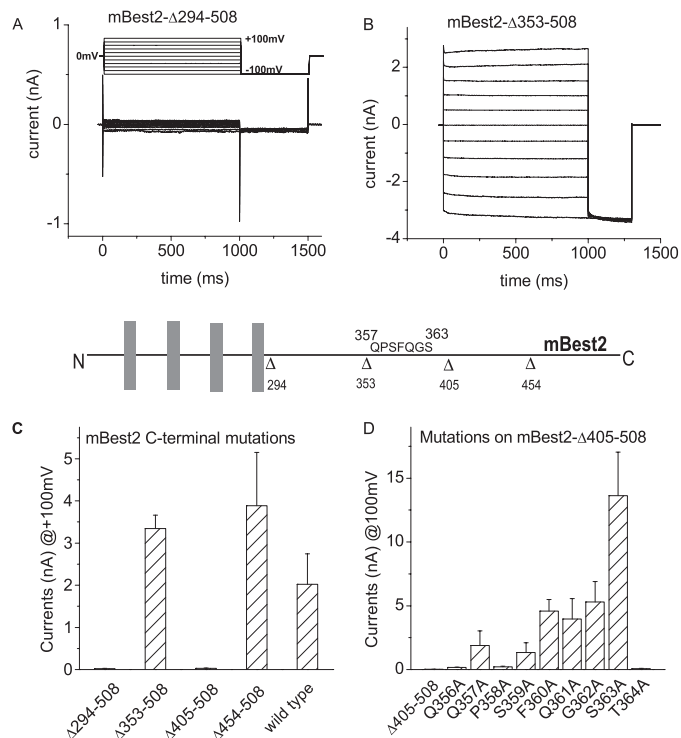


**FIGURE 6. Determination of mBest2 AI domain.** mBest2 mutants were expressed in HEK293 cells for whole-cell recordings as described in Fig. 1. *A*, current traces of mBest2- $\Delta$ 294-508. *B*, current traces of mBest2- $\Delta$ 353-508. *C*, average current amplitudes for different truncation mutants of mBest2. L294X( $\Delta$ 294-508) and V405X( $\Delta$ 405-508) mutations inactivated mBest2 channel ( $p < 0.01$ ), whereas F353X( $\Delta$ 353-508) and S454X( $\Delta$ 454-508) mutations remained functional ( $p > 0.05$  in comparison with wild-type). *D*, average current amplitudes of currents induced by expression of point mutants of mBest2- $\Delta$ 405-508. Compared with  $\Delta$ 454-508 mutant, Q357A and S359A ( $p < 0.05$ ), F360A, Q361A, G362A, and S363A ( $p < 0.01$ ) significantly activated the mBest2- $\Delta$ 405-508 mutant channel.  $n = 4-6$  for *C* and *D*.

## Regulation of Bestrophin Cl<sup>-</sup> Channel Activation

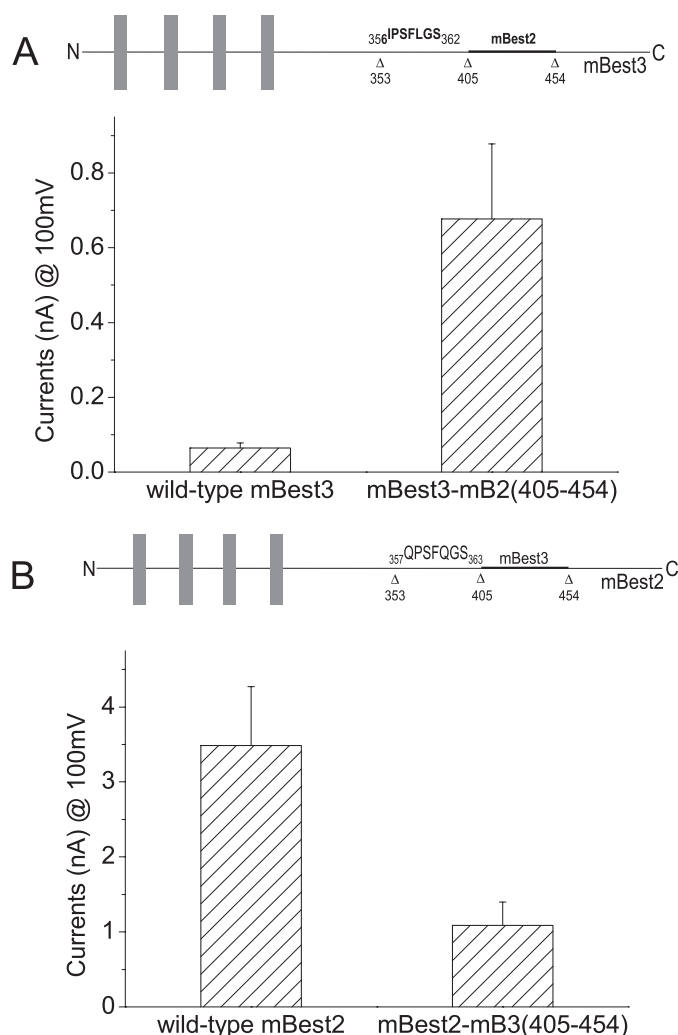


**FIGURE 7. Introduction of the mBest2 facilitatory region (residues 405-454) activated the mBest3 channel.** Regions containing the facilitatory domain (405-454) were swapped between mBest2 and mBest3 (*upper panels* in *A* and *B*). The mBest3-mB2-(405-454) or mBest2-mB3-(405-454) mutant was transfected into HEK293 cells for expression and whole-cell recording as described in Fig. 1. *A*, introduction of the mBest2 residues 404-454 into mBest3 significantly activated the mutant channel, compared with the wild-type mBest3 ( $p < 0.05$ ,  $n = 7-8$ ). *B*, introduction of mBest3 residues 404-454 reduced mBest2 channel activity ( $p = 0.01$ , compared with the wild-type;  $n = 7-8$ ).

is not clear yet, the data indicate that the AI domain is membrane-associated and regulates the channels via association with the channel pore or gating mechanism.

### Potential Mechanisms for the Inhibitory Function of the AI Domain

*AI Domain May Be Associated with Either the Channel Pore or the Gating Machinery*—From the membrane biotinylation result, we concluded that inactivation of mBest3 occurs at the plasma membrane because wild-type mBest3 proteins were detected at the plasma membrane surface (Fig. 2). Supporting this conclusion, we also found that mBest3 AI domain is probably membrane-associated. The membrane association is indicated by hydrophathy analysis but also by protein biochemistry (Fig. 4). When the AI domain is intact, the C-terminal protein was mainly distributed in the particulate or membrane fraction,

## Regulation of Bestrophin Cl<sup>-</sup> Channel Activation

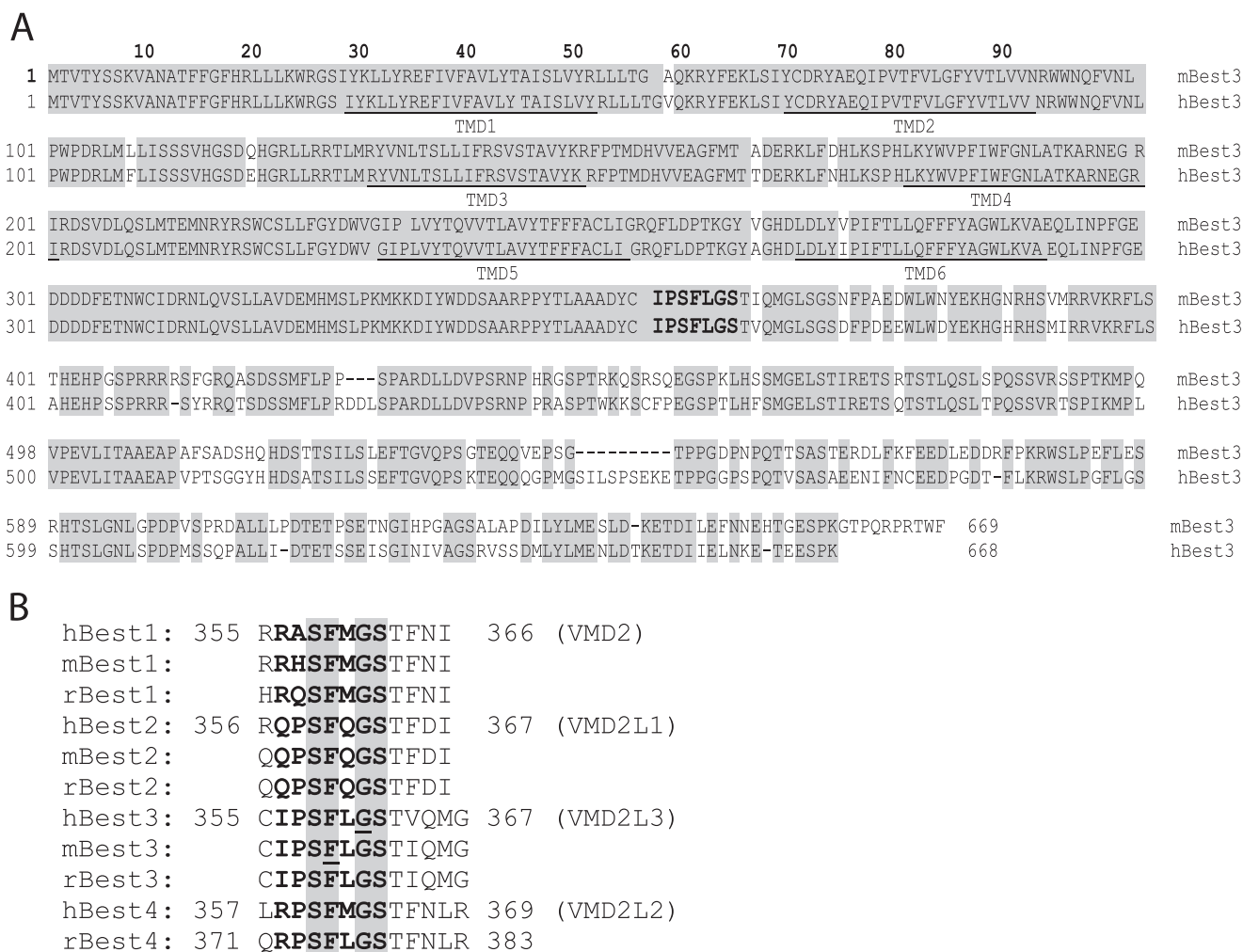


**FIGURE 8. Alignment of bestrophin sequences.** The bestrophin sequences were aligned with ClustalW algorithm. Identical amino acids are shaded. Amino acids in boldface type represent AI domains or the sequences homologous to the AI domains. *A*, alignment of mBest3 and hBest3. Six TMDs predicted by the PMEx program are underlined. GenBank™ accession numbers are as follows: mBest3, AY450426; hBest3, NM\_017682. *B*, alignment of human (*h*), mouse (*m*), and rat (*r*) bestrophin sequences homologous to Best3 AI domains and their flanking sequences. Underlined *G* and *F* are two residues that induced voltage-dependent currents when mutated to alanines.

whereas the C terminus became soluble when a short sequence, including the AI domain, was deleted. We hypothesize that the AI domain plays an inhibitory role as a blocker to block the channel pore from the cytoplasmic side via interacting with a hydrophobic receptor, such as the inner side of TMD2, which was demonstrated as the potential pore structure in mBest2 (15). This hypothesis is supported by our previous results (1). The expression of a wild-type mBest3 C terminus blocked the functional mBest3(Δ353–669) mutant-induced currents in HEK293 cells, but an AI domain-deleted mBest3 C-terminal mutant, 292–669(Δ353–404), did not reduce mBest3(Δ353–669) currents, suggesting that the AI domain may inactivate the bestrophin channel as a physiological channel pore blocker.

Evidence that the AI domain may be involved in channel gating is provided by the finding that certain point mutations in the AI domain (e.g. mBest3-F359A and hBest3-G361A) made the currents voltage-dependent (Fig. 3). Although the AI domains of mBest3 and hBest3 have identical residues, it was surprising that different residues in hBest3 and mBest3 produced voltage-dependent currents. It is possible that amino

acids outside the AI domain introduce a subtle shift in the tertiary structure of the AI domain. After the AI domain, there is only 67% identity between mBest3 and hBest3, whereas between the last TMD and the AI domain there is complete identity. We presume that differences in the C terminus after the AI domains may influence, in different ways, the association of the AI domain with the channel pore or gating mechanism.

*The AI Domain Is a Potential Target Site for Protein Kinase C or PDK1*—To elucidate how the residues in the AI domain regulate the activation of the channel, we searched consensus sites in the mBest2 C terminus by Scansite. Potential protein kinase C phosphorylation sites were found in mBest2 (AFLQ**QPSFQGST**FD; boldface letters represent the AI domain, and the phosphorylation site is underlined.). Further search revealed a potential PDK1 (phosphoinositide-dependent kinase 1)-binding site, AADY**CIP**S**F**L**G**STIQ (mBest3) or **QPSFQGST**F-DIALA (mBest2) around the phosphorylation sites. PDK1 plays a central role in activating AGC kinases (cAMP-dependent protein kinase, protein kinase G, and protein kinase C) (16). This implies that the bestrophin channel function may be regulated by protein phosphorylation of the AI domain.

### The AI Domains Are Relatively Conserved among Human and Murine Bestrophins

Among the vertebrate bestrophins, four residues within the AI domain are very highly conserved. The consensus sequence is SF(M/Q/L)GS (Fig. 8B). This domain follows a highly conserved proline-rich region that is likely to be a region of protein-protein interaction. The residues flanking this consensus sequence vary distinctly among the four bestrophin isoforms. The sequences flanking the consensus are (R/H)RX( . . . )TFNI in Best1, (Q/R)QP( . . . )TFDI in Best2, CIP( . . . )TXQMG in Best3, and RP( . . . )TFNLR in Best4, where ( . . . ) represents SFXGS. We have clearly demonstrated that this region has a functional consequence (AI domain) in both mBest2 and mBest3/hBest3, although their residues are not identical. Our results strongly suggest that the AI domains in the three bestrophins have similar inhibitory functions. It will be interesting to know if those domains in hBest1 and hBest4 also play an inhibitory role similar to Best2 and Best3. Interestingly, two residues in the AI domains of hBest3 and mBest3 (Fig. 8B, *underlined G and F*), which induce voltage-dependent currents when mutated to alanines, belong to the rigorously conserved residues.

### mBest2 Channel Activity May Be Determined by the Competition between the AI and the Facilitatory Domains

Besides the AI domain, there is a region in mBest2 (residues 405–454) that has a facilitatory effect. In mBest2, we hypothesize that the channel activity may be determined by the mutual competition between the AI domain and a facilitatory domain(s) located within the region bounded by the residues 405 and 454. When a stop codon was introduced at the position of 405, the mBest2 mutant ( $\Delta 405$ –508) lost channel function because of the effect of the AI domain was not opposed by the stimulatory domain (Fig. 6 C and D). Point mutations in the AI domain activated the deletion mutant, indicating that the AI domain was responsible for the inhibition when the facilitatory region (405–454) is removed. When the protein was truncated at position of 454 ( $\Delta 454$ –508), the protein behaved as an active Cl<sup>-</sup> channel similar to wild-type mBest2, indicating that residues 405–454 overpowered the inhibitory role of the AI domain and made the channel active. The facilitatory effect became prominent when the AI domain was inactivated by mutation. The facilitatory domain increased the channel activity by ~8-fold when the inhibitory effect of the AI domain is

eliminated (Fig. 5). At present, we do not know if the two domains compete with each other through direct interaction or via associating with a third structure.

Additionally, what is more interesting about the mBest2 facilitatory domain is that its introduction into mBest3 can turn the channel from a nonfunctional into a functional one. This result further supports that the residues 405–454 of mBest2 is a functional facilitator in bestrophin channel activation. Does this region facilitate the channel activity through binding directly to the channel pore, or via interacting with the AI domain, or via some cellular factors? The mechanism by which the mBest2 facilitatory domain enhances the bestrophin channel activity will be an interesting subject to study.

### REFERENCES

1. Qu, Z., Cui, Y., and Hartzell, H. C. (2006) *FEBS Lett.* **580**, 2141–2146
2. Qu, Z., Fischmeister, R., and Hartzell, C. (2004) *J. Gen. Physiol.* **123**, 327–340
3. Qu, Z., and Hartzell, C. (2004) *J. Gen. Physiol.* **124**, 371–382
4. Qu, Z., Wei, R. W., Mann, W., and Hartzell, H. C. (2003) *J. Biol. Chem.* **278**, 49563–49572
5. Sun, H., Tsunenari, T., Yau, K. W., and Nathans, J. (2002) *Proc. Natl. Acad. Sci. U. S. A.* **99**, 4008–4013
6. Tsunenari, T., Sun, H., Williams, J., Cahill, H., Smallwood, P., Yau, K. W., and Nathans, J. (2003) *J. Biol. Chem.* **278**, 41114–41125
7. Kramer, F., Stohr, H., and Weber, B. H. (2004) *Cytogenet. Genome Res.* **105**, 107–114
8. Petrukhin, K., Koisti, M. J., Bakall, B., Li, W., Xie, G., Marknell, T., Sandgren, O., Forsman, K., Holmgren, G., Andreasson, S., Vujic, M., Bergen, A. A., McGarty-Dugan, V., Figueroa, D., Austin, C. P., Metzker, M. L., Caskey, C. T., and Wadelius, C. (1998) *Nat. Genet.* **19**, 241–247
9. Stohr, H., Marquardt, A., Nanda, I., Schmid, M., and Weber, B. H. (2002) *Eur. J. Hum. Genet.* **10**, 281–284
10. Marquardt, A., Stohr, H., Passmore, L. A., Kramer, F., Rivera, A., and Weber, B. H. (1998) *Hum. Mol. Genet.* **7**, 1517–1525
11. Chien, L. T., Zhang, Z. R., and Hartzell, H. C. (2006) *J. Gen. Physiol.* **128**, 247–259
12. Barro Soria, R., Spitzner, M., Schreiber, R., and Kunzelmann, K. (2006) *J. Biol. Chem.*
13. Pifferi, S., Pascarella, G., Boccaccio, A., Mazzatenta, A., Gustincich, S., Menini, A., and Zucchelli, S. (2006) *Proc. Natl. Acad. Sci. U. S. A.* **103**, 12929–12934
14. Neher, E. (1992) *Methods Enzymol.* **207**, 123–131
15. Qu, Z., Chien, L. T., Cui, Y., and Hartzell, H. C. (2006) *J. Neurosci.* **26**, 5411–5419
16. Mora, A., Komander, D., van Aalten, D. M., and Alessi, D. R. (2004) *Semin. Cell Dev. Biol.* **15**, 161–170
17. Qu, Z., Cui, Y., and Hartzell, C. (2007) *FEBS Lett.* **581**, 580